Bulletin of the Seismological Society of America, Vol. 86, No. 3, pp. 646–654, June 1996

Analysis of Spectral Ratios for Estimating Ground Motion in Deep Basins

by M. Dravinski, G. Ding, and K.-L. Wen

Abstract Use of Nakamura's spectral ratio (horizontal versus vertical components) is investigated theoretically for deep sedimentary basins by considering semi-circular and semi-spherical valleys. The ratio is evaluated from the steady-state surface response for different incident waves. Based on this ratio, both the resonant frequencies and ground motion amplification are determined. The results based on Nakamura's ratio are compared with those based on the sediment-to-bedrock spectral ratios (Kagami's ratio).

The results show that for both two- and three-dimensional models, Nakamura's technique predicts well the fundamental resonant frequency, but it could not determine higher resonant frequencies of the basins. The error in Nakamura's estimate of the fundamental resonant frequency increases for stations near the valley center. For alluvial valleys considered in this article, Nakamura's ratio failed to predict accurately surface ground-motion amplification.

Introduction

Local site response atop sedimentary basins can be determined either theoretically or experimentally. Theoretical approach permits parametric analysis of the problem. However, the method requires detailed description of the subsurface geology and sources, and it is characterized by considerable complexities for realistic sedimentary basins (Dravinski *et al.*, 1991). Experimental methods rely on measurements of strong ground motion at sediment sites that are then compared to a "reference" bedrock site response in order to estimate the relative amplification (Lermo *et al.*, 1988). The advantage of this approach is that it does not require detailed subsurface geological structure of the basin. Still, there are considerable difficulties with this method as well. Namely, since local site effect can change considerably within a short distance (Aki, 1988), ground-motion records must be obtained at multiple sites throughout the basin. Consequently, simultaneous strong ground motion recordings at an array of sediment sites and a reference bedrock site for multiple seismic events may be difficult to achieve, especially in regions with moderate to low seismicity.

An alternative experimental approach is to utilize records of ambient seismic noise. For periods greater than 2 sec, the seismic noise is usually categorized as microseisms, and for short periods, as microtremors. Ewing *et al.* (1957) divided the problem of microseisms into four parts: nature of the source, mechanism of transmission over oceanic paths, effects of continental margin, and the type of propagation over continental paths. As for the source, Hasselmann (1963) showed that microseisms can be generated through the action of ocean waves on the coast, change of atmospheric pressure variations over the ocean, and nonlinear interactions between ocean waves. Analysis of transmission over oceanic paths shows that ocean areas beyond the continental margins transmit microseisms poorly and that large microseisms occur only when the portion of storm (or its swell) reaches shallow water (Ewing *et al.*, 1957). The continental margin was found to favor microseism propagation toward the continent rather than toward the ocean (Gutenberg, 1951). The mechanism of microseism propagation over continental paths is one aspect of the microseisms problem that is best understood. In this region, microseisms propagate as *Lg* and *Rg* phases (Ewing *et al.*, 1957).

Short-period microtremors, on the other hand, may consist of both body and surface waves. However, sometimes it is found that they consist mainly of Rayleigh waves excited locally near the recording site (Nogoshi, 1978; Lermo and Chávez-Garcia, 1994; Yamanaka *et al.*, 1994). As the microtremors' period decreases, their dependence on the local sources increases, making it very difficult to interpret their variations from site to site (Aki, 1988).

Presently, there are still major problems in interpretation of both microseisms and microtremors. Still, use of seismic noise in estimating ground-motion amplification is attractive since it can be recorded daily at multiple sites. Consequently, numerous studies have attempted to use it in order to investigate the site effects. Kagami *et al.* (1982, 1986) and Yamanaka *et al.* (1993, 1994) investigated the problem by measuring microseisms while Kobayashi *et al.* (1986), Lermo *et al.* (1988), Lermo and Chávez-Garcia (1994), and Field *et al.* (1990) considered the same problem using microtremors. From these investigations, it is apparent that seismic noise may be an effective tool to determine the predominant period of motion (Kobayashi *et al.,* 1986; Lermo *et al.,* 1988). It is considerably more difficult to infer from it the amplification of ground motion (Gutierrez and Singh, 1992). Further research is needed to settle the question of applicability of seismic noise in estimation of site effects.

Methods for Ground-Motion Amplification Using Seismic Noise

Three different approaches are commonly used to estimate ground-motion amplification of microtremors and microseisms: (1) direct computation of amplitude spectra at sediment sites, (2) evaluation of sediment-to-bedrock spectral ratio for horizontal components of motion (Kagami's ratio), and (3) calculation of spectral ratios between horizontal and vertical components of motion at the same site (Nakamura's ratio). Since spectral amplitude, in addition to site effect, incorporates source and path effects, it is used only to qualitatively assess ground-motion amplification. More precise site-effect estimates are obtained in terms of spectral ratios.

Kagami *et al.* (1982, 1986) proposed that the ratio of the horizontal components of the velocity spectra at the sediment site to those at the rock site can be used as a measure of microseism ground-motion amplification (Kagami's ratio). This proposition assumes a common source and similar paths for sediment and bedrock sites. Therefore, Kagami's ratio is defined as

$$K_{sb} = \frac{H_s}{H_b}, \tag{1}$$

where (H_s, V_s) and (H_b, V_b) denote Fourier spectral amplitude for horizontal and vertical components of motion at sediment site and the reference site, respectively.

Nakamura (1989) proposed a hypothesis that microtremor site effects can be determined by simply evaluating spectral ratio of horizontal versus vertical components of motion observed at the same site. The method implies the following assumptions (Lermo and Chávez-Garcia, 1994; Lachet and Bard, 1994): microtremors consist of Rayleigh waves propagating in a single layer over a half-space, the motion is entirely due to local sources and all deep sources are neglected, and local sources do not affect microtremor motion at the base of the soil layer. Consider now an estimate of site effect of interest in earthquake engineering given by $S_E(\omega) = H_s(\omega)/H_b(\omega)$. Since in addition to body waves microtremors contain surface waves, it is necessary to make corrections to remove the effect of surface waves. Nakamura (1989) assumes that the effect of Rayleigh waves is included in the vertical spectrum at the surface (V_s) and not at the base ground (V_b) and consequently that it can be defined as $A_s(\omega) = V_s(\omega)/V_b(\omega)$. In order to compensate S_E by the source spectrum, a modified site-effect spectral ratio is defined by $S_M(\omega) = S_E(\omega)/A_s(\omega) = (H_s/V_s)/(H_b/V_b)$. Nakamura (1989) demonstrated experimentally using records from a borehole that if microtremors consist mainly of Rayleigh waves, then the assumption

$$\frac{H_b(\omega)}{V_b(\omega)} \approx 1 \tag{2}$$

is nearly valid for a relatively wide frequency range, and the modified site-effect spectral ratio becomes

$$S_m(\omega) \approx \frac{H_s(\omega)}{V_s(\omega)} = N_s(\omega). \tag{3}$$

Therefore, Nakamura (1989) concluded that the spectral ratio between horizontal and vertical components for microtremors can be used as an estimate of the site effect for body waves. Equation (2) is the so-called Nakamura's hypothesis, and the ratio given by equation (3) is known as Nakamura's ratio. Nakamura's estimate appears attractive since it eliminates the problem of source and path effects. However, at this point, the validity of Nakamura's estimate has not been completely established, especially for deep sedimentary basins.

Field and Jacob (1993) modeled microtremors by considering a three-dimensional model consisting of a single elastic layer over a half-space subjected to random distribution (in space and time) of point forces located on top of the layer. The random forces were to represent microtremor sources. Using the Green's function approach, horizontal and vertical spectral amplitudes were evaluated at the top surface of the layer. Nakamura'cs ratio was calculated as a function of frequency and then compared with the surface response spectra for vertically incident plane *SH* waves. It was found that the frequency of the most prominent peak, in both horizontal-component noise spectrum and Nakamura's ratio, agrees with the fundamental resonant frequency for vertically incident shear waves. The peak of horizontal noise spectrum was shifted slightly ($\approx$10%) toward higher frequencies relative to the peak in Nakamura's ratio. The peak amplification in Nakamura's estimate was found to be $\approx$1.5 times that of the earthquake response. Attempts to compare relative noise amplitudes between sediment and rock sites were unsuccessful.

Recently, Lermo and Chávez-Garcia (1994) modeled microtremors as Rayleigh waves propagating in a layer over a half-space. Nakamura's ratio and hypothesis were examined for this model. The results show that the underlying assumptions of Nakamura's technique are consistent with propagation of Rayleigh waves.

Similarly, Lachet and Bard (1994) investigated numerically and theoretically the applicability of Nakamura's technique by considering single-station recordings of horizontally stratified medium when subjected to random noise sources. They concluded that Nakamura's method can be used to determine the fundamental resonance frequency of a given sediment site but that it failed to predict the amplification of surface ground motion. Furthermore, they showed that the fundamental resonant frequency obtained through Nakamura's ratio using noise simulation was independent of the source excitation function and that the ratio is largely controlled by the polarization curve of fundamental Rayleigh waves. Yamanaka *et al.* (1994) investigated applicability of microseisms in inferring subsurface structure by measuring them in the Kanto Plain, Japan. They found that Nakamura's ratio (ellipticity) at each site is stable with time. Good agreement was found between Nakamura's ratio at a sediment site and the same ratio computed for Rayleigh waves in which the structure of the sediment beneath the site was taken into account. They showed that Nakamura's ratio for Rayleigh waves in earthquake ground motions was consistent with that of microtremors. These results provide strong evidence that microseisms in the area studied consist mainly of Rayleigh waves. The subsurface structure was deduced by trial-and-error fitting of observed Nakamura's ratio with corresponding theoretical ratios calculated assuming Rayleigh waves. The results suggest that Nakamura's ratio from microseisms may be used in some cases for deducing subsurface structure.

The above studies did not address the problem of dipping layer structure of sedimentary basins. For that purpose, the validity of Nakamura's approach is examined next for deep sedimentary basins. Two models are considered: a two-dimensional valley (plane strain model for a semi-cylindrical shape) and a three-dimensional valley (a semi-spherical shape).

Since the spectral ratios in addition to ground-motion amplification allow estimation of the sediment resonant frequencies (Lermo *et al.*, 1988), this study will address both by using Kagami's and Nakamura's ratios.

Methods of Solution

Calculations of surface response spectra for deep sedimentary basins are based on boundary integral equation (BIE) methods (Dravinski and Mossessian, 1987; Mossessian and Dravinski, 1990; Eshraghi and Dravinski, 1989).

The resonant frequencies, on the other hand, are evaluated using two different methods: an eigenvalue method of Zhou and Dravinski (1994) and a spectral search method. A brief outline of the eigenvalue method is presented next.

Resonant Frequencies Based on an Eigenvalue Method

The geometry of the general three-dimensional problem is depicted by Figure 1. A sedimentary valley D is perfectly embedded in an elastic half-space D_0 along the interface S_I. The surface of the half-space is marked by S_F. (Throughout, the variables with subscript 0 correspond to the half-space.) The density, S-, and P-wave velocities are denoted by ρ, β, and α, respectively, while ν and μ describe Poisson's ratio and shear modulus, respectively. Impedance contrast I_β and dimensionless frequency Ω are defined according to (Zhou and Dravinski, 1994):

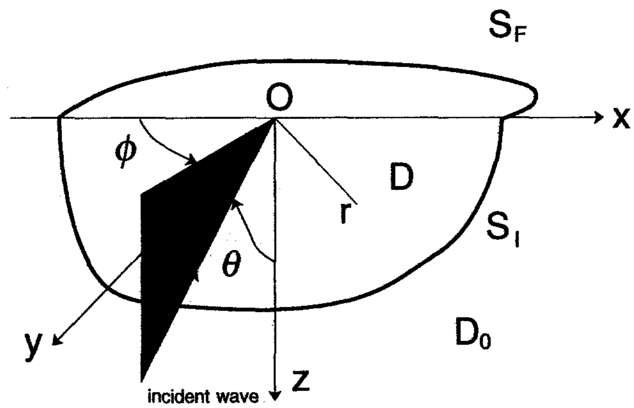

Figure 1. Geometry of the general model: an alluvial valley D embedded within an elastic half-space D_0. S_F: surface of the half-space; S_I: the valley-bedrock interface; ϕ: azimuthal angle; θ: off-vertical angle; ϕ_{inc}, θ_{inc}: azimuthal and off-vertical angles of incidence.

$$I_\beta = \frac{\rho_0 \beta_0}{\rho \beta}, \tag{4}$$

$$\Omega = \frac{f}{f_h^s} = \frac{2kh}{\pi}, \tag{5}$$

$$f_h^s = \frac{\beta}{4h}, \tag{6}$$

where h is the maximum depth of the valley, k is the shear wavenumber, and β denotes the shear-wave velocity. Here, f_h^s is the fundamental frequency of a flat layer, with thickness h corresponding to a vertical S-wave incidence. It should be noted that for geophysical problems, the impedance contrast is greater than one; i.e., $I_\beta > 1$. Throughout the article, Ω_1 denotes the fundamental resonant frequency, and Ω_i, $i = 2, 3, \ldots$, represent higher-order frequencies.

The wave fields in the valley and the half-space satisfy the following equations of motion and boundary conditions:

$$(\lambda + \mu)\nabla\nabla \cdot \mathbf{u} + \mu\nabla^2\mathbf{u} + \rho\omega^2\mathbf{u} = 0, \quad \mathbf{x} \in D; \tag{7}$$

$$(\lambda_0 + \mu_0)\nabla\nabla \cdot \mathbf{u}_0 + \mu_0\nabla^2\mathbf{u}_0 + \rho_0\omega^2\mathbf{u}_0 = \mathbf{0}, \quad \mathbf{x} \in D_0; \tag{8}$$

$$\mathbf{t}^n = \mathbf{t}_0^n = 0, \quad \mathbf{x} \in S_F; \tag{9}$$

$$\mathbf{t}^n = \mathbf{t}_0^n, \quad \mathbf{u} = \mathbf{u}_0, \quad \mathbf{x} \in \mathbf{S}_I; \tag{10}$$

where $\mathbf{x} = (x, y, z)$ is the position vector, $\mathbf{u} = (u, v, w)$ is the displacement vector, λ and μ are the Lamé constants, $\mathbf{t}^n$ is a traction vector along the unit normal $\mathbf{n}$ of the surface S_F or S_I (Fig. 1), and ω is the circular frequency. The steady-state solution is obtained by using an indirect boundary integral equation method (Dravinski and Mossessian, 1987).

Zhou and Dravinski (1994) have shown that the resonant frequencies for the valley correspond to the eigenvalues of the problem involving equations of motion (7), with stress-free boundary conditions (9), and rigid displacement boundary conditions:

$$\mathbf{u} = \mathbf{0}, \quad \mathbf{x} \in S_I. \tag{11}$$

The key features of the resonant frequencies are summarized as follows: (1) They are properties of the valley and not the incident waves; i.e., the valley resonance takes place at the same frequencies for different incidence although some modes may not be excited by a particular incident wave. (2) The dimensionless resonant frequencies are independent of the impedance contrast I_β between the valley and the half-space. (3) The resonant frequencies correspond to the eigenfrequencies of the eigenvalue problem defined by equations (7) through (11).

Resonant Frequencies Based on Spectral Search Method

The valley resonant frequencies can be determined using spectral search methods as well. This requires steady-state solution of the problem for a range of frequencies and different incident waves. Since the displacement field has in general three components of motion that may be out of phase across the top surface S_F (Fig. 1), it is insufficient to consider only one component of motion in order to identify the resonant frequencies. Instead, the total surface displacement amplitude of the inclusion should be used. Furthermore, for a particular incidence, some modes of motion may not be excited, therefore several incident waves must be considered to excite all the modes in the range of frequency of interest. Finally, in order to avoid possible nodal points, it is necessary to calculate the surface response at multiple locations. Once the spectral amplitudes are calculated for a set of observation points along the valley surface S_F, it is possible to construct a histogram of all the spectral peaks as a function of frequency in order to determine the resonant frequencies.

Resonant Frequencies Results

Two-Dimensional Problem

For this model, the valley is of semi-circular shape of unit radius. For the plane strain model, the motion takes place in the $y = 0$ plane; i.e., the displacement vector field is described by $\mathbf{u} = (u, 0, w)$, where u and w denote displacement components along the x and z axes, respectively.

Two-Dimensional Frequencies Based on Eigenvalue, Spectral Search, and Kagami's Ratio Methods

Using the eigenvalue approach, Zhou and Dravinski (1994) found the first four resonant frequencies to be as follows: $\Omega_1 = 2.15$, $\Omega_2 = 2.25$, $\Omega_3 = 2.67$, and $\Omega_4 = 3.25$.

Through the spectral search method based on an indirect BIE approach (Dravinski and Mossessian, 1987), a histogram of all spectral peaks is evaluated, as shown by Figure 2. Nine incident plane harmonic waves are considered: *P*, *SV* ($\theta_{inc} = 0°$; 30°; 60°, and 85°) and a Rayleigh wave. From this histogram, the first four dimensionless resonant frequencies are determined to be $\Omega_1 = 2.0$, $\Omega_2 = 2.2$, $\Omega_3 = 2.6$, and $\Omega_4 = 3.3$. Therefore, the resonant frequencies based on the eigenvalue method and the spectral search method are summarized in Table 1.

Apparently, the results based on the two methods are in good agreement. It is interesting to point out that sediment-bedrock spectral ratios can be used to produce a "sharper estimate" of fundamental resonant frequency than the one obtained through the spectral amplitude approach. To illustrate this, Kagami's ratio is evaluated for a set of sediment sites and incident Rayleigh waves. The ratio for three sedi-

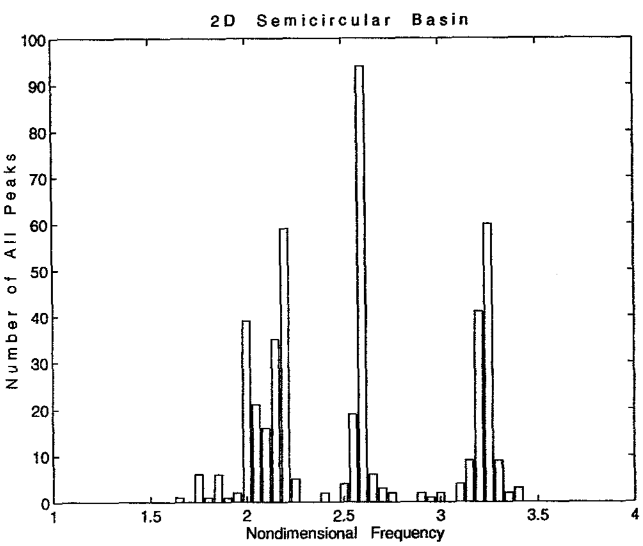

Figure 2. Histogram of maximum peaks for surface displacement spectral amplitude for a semi-circular valley of unit radius embedded in an elastic half-space (plane strain model). Nine plane harmonic incident waves are considered (Rayleigh wave and *P* and *SV* waves with angles of incidence 0°, 30°, 60°, and 85°). The response is evaluated at 21 equally spaced stations along the valley surface S_F. Unless stated differently, the following parameters are assumed: $\beta = 1/2$; $a = 1$, $\nu = 1/3$, $\mu = 1/16$, $\beta_0 = 1$, $a_0 = 2$, $\nu_0 = 1/3$; $\mu_0 = 1$, $I_\beta = 8$.

Table 1
Resonant frequencies of different order for a semi-cylindrical valley of unit radius based on eigenvalue method (EM) (after Zhou and Dravinski, 1994) and the spectral search method (SSM).

	Ω_1	Ω_2	Ω_3	Ω_4
EM	2.15	2.25	2.67	3.25
SSM	2.0	2.2	2.6	3.3

ment sites and the reference bedrock site (1, 0, 0) is displayed in Figure 3. Fundamental resonant frequency $\Omega_1 = 2.15$ can be determined for all three sediment sites, confirming the fundamental frequency calculations based on the eigenvalue and spectral amplitude methods. It should be noted that while the second resonant frequency (Ω_2) can be observed as well, the third resonant frequency (Ω_3) is not excited by this incident wave, and consequently, it does not appear in Figure 3.

From the presented results, it is evident that for the theoretical model, the eigenvalue, spectral search, and Kagami's ratio methods all provide the exact value of the fundamental resonant frequency. Nakamura's estimate of the resonant frequencies for the same model is considered next.

Two-Dimensional Frequencies Based on Nakamura's Estimates

The implicit assumption in Nakamura's approach is that the microtremors consist mainly of Rayleigh waves (Nakamura, 1989). This has been observed by Lermo and Chávez-Garcia (1994) for microtremors in three cities in Mexico and by Yamanaka *et al.* (1994) for microseisms in Kanto Plain in Japan. Therefore, Nakamura's ratio for a semi-circular alluvial valley is evaluated for incident Rayleigh waves only. Figure 4 depicts this ratio for three sediment sites. The fundamental resonant frequency is clearly identified only for the site near the edge of the valley. In order to clarify this phenomenon, Kagami's and Nakamura's ratios are evaluated for 10 sites located between the center and the edge of the valley. From these results, the fundamental resonant frequency estimates based on the two ratios are presented in Table 2.

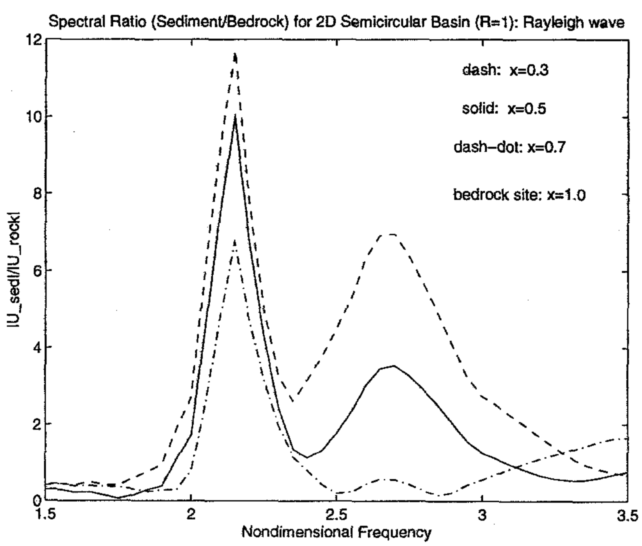

Figure 3. Kagami's ratio U_s/U_b for a semi-circular alluvial valley of unit radius and incident plane harmonic Rayleigh wave for three sediment sites (x, 0, 0). The sediment sites are located at (0.3, 0, 0), (0.5, 0, 0), and (0.7, 0, 0). Reference bedrock site: (1, 0, 0).

Here, x denotes the x coordinate of different stations (x, 0, 0) at the surface of the half-space, while the superscripts K and N correspond to Kagami's and Nakamura's estimates, respectively.

It is evident from Table 2 that Nakamura's estimate for first resonant frequency is more accurate near the valley's edge than near the center of the valley. The higher-order frequencies, on the other hand, are not consistently predicted by this ratio. The error in Nakamura's estimate results in downward shift of the fundamental frequency. For the site at the center of the valley, this shift is about 7%. Field and Jacob (1993) reported a 10% shift in resonant frequencies when using Nakamura's estimate.

From the presented results, it appears that for deep two-dimensional sedimentary basins, the fundamental resonant frequency determined through Nakamura's ratio agrees well

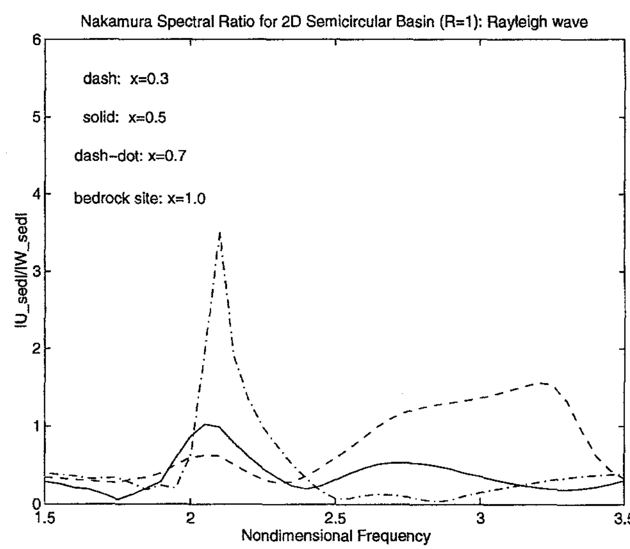

Figure 4. Nakamura's ratio U_s/W_s as a function of frequency for three sediment sites on the surface of a semi-circular alluvial valley subjected to incident plane harmonic Rayleigh wave. Sediment sites are located at (0.3, 0, 0), (0.5, 0, 0), and (0.7, 0, 0).

Table 2

Fundamental resonant frequency for a semi-circular valley of unit radius subjected to an incident Rayleigh wave based on Kagami's and Nakamura's ratios for 10 surface sites (x, 0, 0).

x	Ω_1^K	Ω_1^N
0	2.15	2.00
0.1	2.15	2.05
0.2	2.15	2.05
0.3	2.15	2.05
0.4	2.15	2.05
0.5	2.15	2.05
0.6	2.15	2.05
0.7	2.15	2.10
0.8	2.15	2.15
0.9	2.15	2.15

with the resonant frequency obtained through the eigenvalue and spectral search methods (with a small downward shift). The accuracy of the resonant frequency estimate based on Nakamura's ratio increases for the sites away from the center of the valley. Higher-order resonant frequencies are not predicted well with this method.

Three-Dimensional Model

The three-dimensional model consists of a semi-spherical valley of unit radius embedded within an elastic half-space $z \geqq 0$ subjected to different incident waves (Fig. 1). Resonant frequencies of the valley are determined using (a) an eigenvalue method (Zhou and Dravinski, 1994), (b) spectral search methods (one based upon surface displacement spectra and the other on sediment-bedrock spectral ratio), and (c) Nakamura's estimate.

Three-Dimensional Frequencies Based on Spectral Search, Eigenvalue, and Kagami's Ratio Methods

For the three-dimensional problem, it is convenient to solve the eigenvalue problem defined by equations (7), (9), and (11) by using the finite-element technique. For that purpose, the finite-element package COSMOS/M, V.1.65A was used. The finite-element mesh incorporated 1695 ten-node tetrahedral elements with a total of 2882 nodes. The first three resonant frequencies are determined to be $\Omega_1 = 2.54$, $\Omega_2 = 2.58$, and $\Omega_3 = 2.86$.

The spectral search methods for the three-dimensional problem utilized BIE techniques (Eshraghi and Dravinski, 1989; Mossessian and Dravinski, 1990a, 1990b). Following Eshraghi and Dravinski (1989), Zhou (1993) determined the resonant frequencies for a semi-spherical valley to be $\Omega_1 = 2.45$, $\Omega_2 = 2.75$, and $\Omega_3 = 2.95$. In this study, the spectral ratio calculations are performed along three rings on the surface of the valley S_F using an indirect BIE method (Mossessian and Dravinski, 1990). The radius R of the rings was assumed to be 0.3, 0.5, and 0.7. Each ring has 36 stations in 10° increments. The reference bedrock site was assumed at (−1.05, 0, 0). Sediment-bedrock spectral ratios were calculated for the resultant displacement field $(U^2 + V^2 + W^2)^{1/2}$ and 10 incident waves [*P*, *SH*, and *SV* waves (with $\theta_{inc} = 0°, 30°$, and 60° and $\phi_{inc} = 0$) and a Rayleigh wave]. From the spectral ratio peaks, the histogram for ring of radius $R = 0.5$ is depicted by Figure 5. Similar histograms were obtained for stations along the other two rings. From these histograms, the dimensionless resonant frequencies are determined to be $\Omega_1 = 2.40$, $\Omega_2 = 2.64$, and $\Omega_3 = 2.88$.

Therefore, the resonant frequencies for the semi-spherical valley obtained through the spectral search, eigenvalue, and spectral ratio methods are summarized in Table 3.

Apparently the first three resonant frequencies obtained by the three different methods agree well. Consequently, the resonant frequencies for a semi-spherical valley are taken to be the average values from the three calculations: $\Omega_1 = 2.46$, $\Omega_2 = 2.66$, and $\Omega_3 = 2.90$. These will be compared with the resonant frequencies based on Nakamura's ratio.

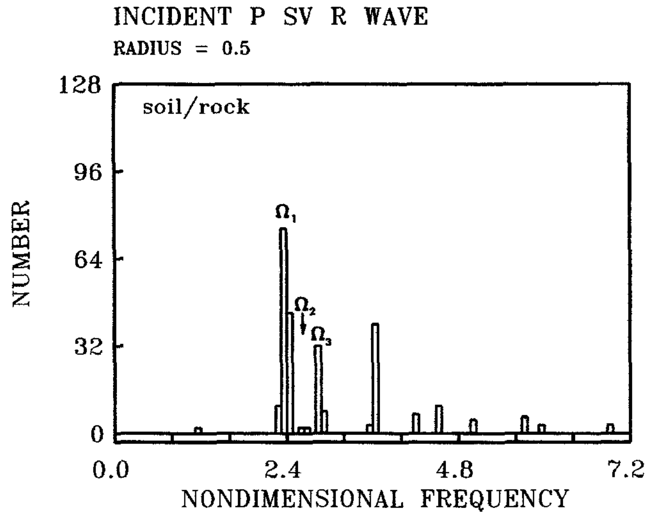

Figure 5. Histogram of the resultant displacement sediment-bedrock spectral ratio peaks for a unit semi-sphere subjected to different plane harmonic incident waves. Reference bedrock site is located at (−1.05, 0, 0). Surface sites along $z = 0$ are placed with 10° increments along a ring of radius $R = 0.5$. Unless stated differently, the material properties of the valley and the half-space are $\alpha = 1$, $\beta = 1/2$, $\nu = 1/3$, $\rho = 1/5$, $\mu = 1/20$ and $\alpha_0 = 2$, $\beta_0 = 1$, $\nu_0 = 1/3$, $\rho_0 = 1$, $\mu_0 = 1$.

Table 3
First three resonant frequencies for a semi-spherical valley based on spectral amplitude (SA; after Zhou, 1993), eigenvalue (EM: 1695 ten-nodes tetrahedral elements with total of 2882 nodes); and spectral ratio (S/R) methods.

i	Ω_i^{SA}	Ω_i^{EM}	$\Omega_i^{S/R}$
1	2.45	2.54	2.40
2	2.75	2.58	2.64
3	2.95	2.86	2.88

Three-Dimensional Frequencies Based on Nakamura's Estimate

Nakamura's ratio *U/W* (horizontal versus vertical spectral amplitude) is calculated for the three rings along the surface of the valley defined earlier. Based on these calculations, corresponding histograms of the main peaks for the *U/W* estimates were evaluated analogously to the sediment-bedrock calculations. The dimensionless fundamental frequencies determined from these histograms are listed in Table 4.

Comparison of the resonant frequencies obtained through the spectral search methods and Nakamura's estimate is shown in Figure 6. Evidently, only the fundamental resonant frequency is accurately predicted using Nakamura's approach for stations away from the valley's center. Near the valley's center, the error in Nakamura's prediction for fundamental resonant frequency increases. Furthermore,

Table 4
Resonant frequencies based on Nakamura"s estimate for a unit semi-sphere and surface sites along three rings of different radius *R*.

R	Ω_1^N	Ω_2^N	Ω_3^N
0.3	2.76	2.96	3.12
0.5	2.60	2.80	2.96
0.7	2.52	2.88	3.68

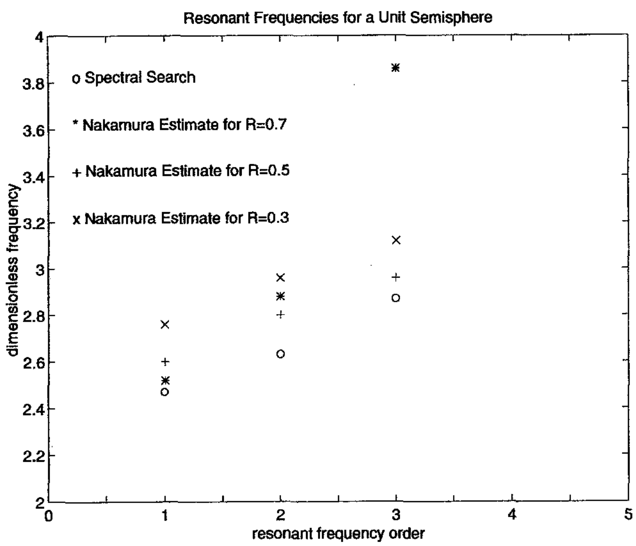

Figure 6. Comparison of the first three resonant frequencies for a unit semi-sphere based on spectral search method (solid circles) and Nakamura's estimate for surface sites along three circles of radii $R = 0.3(\times)$, $0.5(+)$, and $0.7(*)$.

higher-order resonant frequencies are not predicted accurately using Nakamura's approach.

Ground-Motion Amplification

Surface ground-motion amplification at each site is evaluated in terms of Kagami's and Nakamura's spectral ratios for a semi-circular and semi-spherical alluvial valleys. The two ratios are compared for different sites for a range of frequencies.

Two-Dimensional Model

For this model, Kagami's and Nakamura's ratios are evaluated at 10 stations uniformly spaced along the surface of a unit semi-circular valley and incident plane harmonic Rayleigh wave. Reference bedrock site is chosen at station (1, 0, 0). The numerical results for the two ratios are depicted by Figure 7. Apparently, both ratios are strongly frequency dependent. While Kagami's ratio predicts the fundamental resonant frequency accurately for all nine stations, Nakamura's ratio determines the fundamental resonant frequency approximately with the accuracy of the estimate improving for the sites away from the center of the valley. At fundamental resonant frequency, Kagami's ratio increases with increase of sediment depth while Nakamura's ratio decreases. Overall, Nakamura's ratio failed to predict accurately surface ground-motion amplification.

Therefore, two-dimensional results demonstrate that Nakamura's ratio predicts well only the fundamental resonance frequency of the valley. The ratio failed to describe properly surface ground-motion amplification.

Three-Dimensional Model

In order to compare ground-motion amplification in terms of Kagami's and Nakamura's ratios for a semi-spherical valley, the two ratios are evaluated for a range of frequencies at three surface sites (0.3, 0, 0), (0.5, 0, 0), and (0.7, 0, 0) for a unit semi-sphere embedded in a half-space. Reference bedrock site is chosen at station (−1.05, 0, 0), and the incident wave is assumed to be a plane harmonic Rayleigh wave. Numerical results for the two ratios and three-dimensional model are depicted by Figure 8. Apparently, the two ratios are strongly frequency dependent, and they are significantly different from each other for a wide range of frequencies. Therefore, both three- and two-dimensional results show that for the type of valley considered in this article, Nakamura's ratio failed to predict accurately surface ground-motion amplification.

Conclusions

For the valleys considered in this article, both two- and three-dimensional models demonstrate that Nakamura's technique predicts well the fundamental resonant frequency of deep sedimentary basins. The technique is inadequate in determining higher-order resonant frequencies. Presented results show that for stations near the valley center, the error in Nakamura's estimate of the fundamental resonant frequency increases.

As a measure of ground-motion amplification, Nakamura's ratio appears to be inadequate. Its value was significantly different from the corresponding sediment-to-bedrock ratio for a wide range of frequencies. Consequently, while Nakamura's ratio may be a useful tool in estimating the fundamental resonance frequency of the valley, the ratio appears to be inadequate in estimating ground-motion amplification in deep sedimentary basins. The above results are in agreement with those obtained by Lachet and Bard (1994), who investigated the validity of Nakamura's technique in horizontally stratified media.

Acknowledgments

This research was completed through support by an NSF Grant CMS-9412759 and in part through support by an NSF U.S.A.–Taiwan Cooperation Program Grant INT-9021623, and a Southern California Earthquake Center grant. The authors would like to thank Keiiti Aki for several discussions on topics covered in this article and to Pierre-Yves Bard for pointing out an additional reference related to this work. Special thanks go to

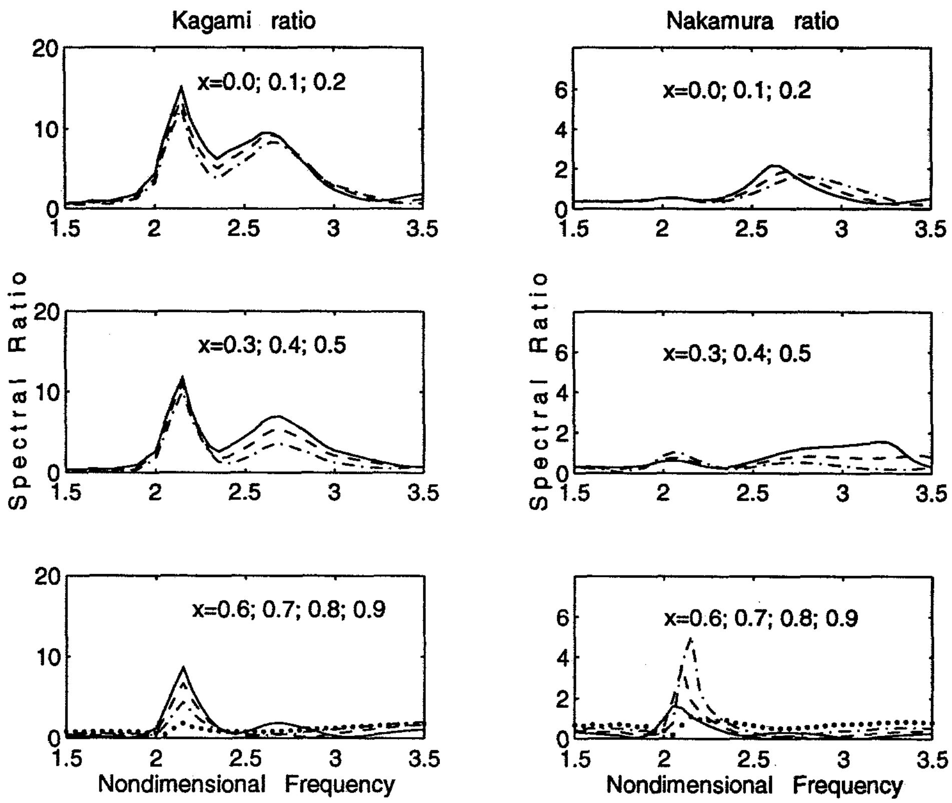

Figure 7. Kagami's and Nakamura's ratios as a function of frequency and position x of observation stations $(x, 0, 0)$ for a semi-circular alluvial valley subjected to incident plane harmonic Rayleigh wave. For each figure, solid, dash, dash dot, and dot line correspond to x in increasing order.

two anonymous reviewers and Art McGarr for their constructive criticism of the article. The assistance in measurements from the people of Kinemetrics, Inc., Pasadena, is greatly appreciated.

References

Aki, K. (1988). Local site effects and strong ground motion, *Proc. Spec. Conf. Earthquake Eng. Soil Dyn.,* A.S.C.E., Park City, Utah.

Dravinski, M. and T. K. Mossessian (1987). Scattering of plane harmonic P, SV, and Rayleigh Waves by dipping layers of arbitrary shape, *Bull. Seism. Soc. Am.* **77,** 212–235.

Dravinski, M., T. K. Mossessian, H. Kagami, and H. Eshraghi (1991). Predominant motion of the Los Angeles sedimentary basin, *Eng. Anal. Boundary Elements* **8,** no. 4, 206–214.

Eshraghi, H. and M. Dravinski (1989). Scattering of elastic waves by nonaxisymmetric three dimensional dipping layer, *Num. Meth. Part. Diff. Eqns.* **5,** 327–345.

Ewing, M., W. S. Jerdetzky, and F. Press (1957). *Elastic Waves in Layered Media,* McGraw-Hill, New York.

Field, E. H., S. E. Hugh, and K. H. Jacob (1990). Using microtremors to assess potential earthquake site response: a case study in Flushing Meadows, New York City, *Bull. Seism. Soc. Am.* **80,** part A, 1456–1480.

Field, E. and K. Jacob (1993). The theoretical response of sedimentary layers to ambient seismic noise, *Geophys. Res. Lett.* **20,** no. 24, 2925–2928.

Gutenberg, B. (1951). Observation and theory of microseisms, *Compendium of Meteorology,* American Meteorological Soc., Boston.

Gutierrez, C. and S. K. Singh (1992). A site effect study in Acapulco, Guerrero, Mexico: comparison of results from strong ground motion and microtremor data, *Bull. Seism. Soc. Am.* **82,** 642–659.

Hasselman, K. (1963). A statistical analysis of the generation of microseisms, *Rev. Geophys.,* **1,** no. 2, 177–210.

Kagami, H., C. M. Duke, G. C. Liang, and Y. Ohta (1982). Observation of 1- to 5-second microtremors and their application to earthquake engineering. Part II. Evaluation of site effect upon seismic wave amplification due to extremely deep soil deposits, *Bull. Seism. Soc. Am.* **72,** no. 3, 987–998.

Kagami, H., S. Okada, K. Shiono, M. Oner, M. Dravinski, and A. K. Mal (1986). Observation of 1- to 5-second microtremors and their application to earthquake engineering. Part III. A two-dimensional study of site effects in the San Fernando Valley, *Bull. Seism. Soc. Am.* **76,** no. 6, 1801–1812.

Kobayashi, H., K. Seo, S. Midorikawa, and S. Kataoka (1986). Measurements of microtremors in and around Mexico D.F., Part I. Technical Report, Tokyo Institute of Technology, Yokohama, Japan, 1986.

Lachet, C. and P.-Y. Bard (1994). Numerical and theoretical investigations on the possibilities and limitations of Nakamura's technique, *J. Phys. Earth* **42,** 377–397.

Lermo, J. and F. J. Chávez-Garcia (1994). Are microtremors useful in site response evaluation?, *Bull. Seism. Soc. Am.* **84,** no. 5, 1350–1364.

Lermo, J. F., M. Rodriguez, and S. K. Singh (1988). The Mexico earthquake of Sept. 19, 1985—Natural period of sites in the valley of Mexico from microtremor measurements and from strong ground motion data, *Earthquake Spectra* **4,** 805–814.

Mossessian, T. K. and M. Dravinski (1990a). Amplification of elastic waves by a three dimensional valley, Part 1: Steady-state response, *Earthquake Eng. Struct. Dyn.* **19,** 667–680.

Mossessian, T. K. and M. Dravinski (1990b). Amplification of elastic waves

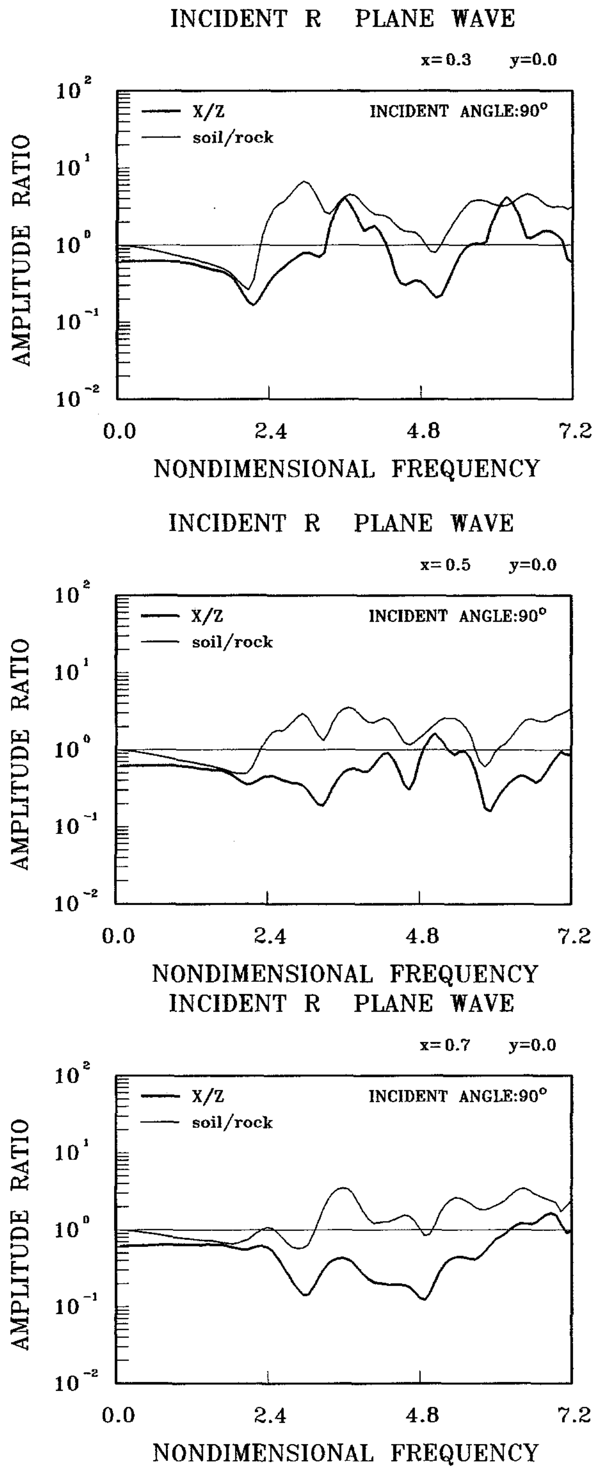

Figure 8. Comparison of Kagami's and Nakamura's ratio for a unit semi-spherical alluvial valley embedded in an elastic half-space and subjected to an incident Rayleigh wave (3D model). Three sites on the surface of the valley are considered: (0.3, 0, 0), top; (0.5, 0, 0), middle; and (0.7, 0, 0), bottom. Reference bedrock site is chosen at (−1.05, 0, 0). Kagami's ratio: thin solid line; Nakamura's ratio: thick solid line.

by a three dimensional valley, Part 2: Transient response, *Earthquake Eng. Struct. Dyn.* **19,** 681–691.

Nakamura, Y. (1989). A method for dynamic characteristics estimation of subsurface using microtremor on the ground surface, *Q. Rept. Railway Tech. Res. Inst.* **30,** no. 1, 25–33.

Nogoshi, M. (1978). On fundamental nature of microtremors, *J. Min. Coll. Akita Univ., Ser. A* **5,** no. 3, 1–51.

Yamanaka, H., M. Dravinski, and H. Kagami (1993). Fundamental characteristics of long period microtremors as observed in the Los Angeles metropolitan area, *Bull. Seism. Soc. Am.* **83,** no. 5, 1595–1609.

Yamanaka, H.,-M. Takemura, H. Ishida, and M. Niwa (1994). Characteristics of long-period microtremors and their applicability in exploration of deep sedimentary layers, *Bull. Seism. Soc. Am.* **84,** no. 6, 1831–1841.

Zhou, T. (1993). Resonance of an elastic inclusion partially embedded in a half-space, *Ph.D. Thesis,* University of Southern California, Los Angeles, California.

Zhou, T. and M. Dravinski (1994). Resonance of sediment valleys and its prediction through an eigenvalue method, *Geophys. J. Int.* **117,** 749–762.

University of Southern California
Los Angeles, California 90089-1453
(M.D., G.D.)

Institute of Earth Sciences
Academia Sinica
P.O. Box 1-55
Taipei, Taiwan
(K.-L.W.)

Manuscript received 21 August 1995.